Received: 15 September 2020 | Revised: 16 January 2021 | Accepted: 24 January 2021

DOI: 10.1111/odi.13785

ORIGINAL ARTICLE

ORAL DISEASES WILEY

Self-assembled peptide hydrogel scaffolds with VEGF and BMP-2 enhanced *in vitro* angiogenesis and osteogenesis

Ruijuan Zhang[1] | Yang Liu[1] | Yingqiu Qi[2] | Ying Zhao[3] | Guangjun Nie[3] | Xiaozhe Wang[1] | Shuguo Zheng[1]

[1]Department of Preventive Dentistry, Peking University School and Hospital of Stomatology, National Clinical Research Center for Oral Diseases, National Engineering Laboratory for Digital and Material Technology of Stomatology, Beijing Key Laboratory of Digital Stomatology, Beijing, PR China

[2]School of Basic Medical Sciences, Zhengzhou University, Zhengzhou, PR China

[3]CAS Key Laboratory for Biomedical Effects of Nanomaterials and Nanosafety, CAS Center for Excellence in Nanoscience, National Center for Nanoscience and Technology, Beijing, PR China

Correspondence
Shuguo Zheng and Xiaozhe Wang, Department of Preventive Dentistry, Peking University School and Hospital of Stomatology, 22 Zhongguancun South Avenue, Haidian District, Beijing 100081, PR China.
Emails: kqzsg86@bjmu.edu.cn; neptunewxz@163.com

Funding information
Peking University School and Hospital of Stomatology Science Foundation for Young Scientists , Grant/Award Number: [PKUSS20170106]

[Correction added on March 16, 2021, after first online publication. The first affiliation and correspondence address were corrected.]

Objectives: The reconstruction of bone defects remains a major clinical issue. Our study aims to investigate the ability of RATEA16 (RA, [CH3CONH]RADARADARADARADA-[CONH2]) for the sustained delivering VEGF and BMP-2 to promote angiogenesis and osteogenesis in bone reconstruction.

Materials and methods: We prepared and investigated the characterization of RATEA16. The survival of human umbilical vein endothelial cells (HUVECs) and human stem cells of the apical papilla (SCAPs) encapsulated in RATEA16 hydrogel was detected. Then, we established RA-VEGF/BMP-2 drug delivery systems and measured their drug release pattern. The effects of RA-VEGF scaffolds on HUVECs angiogenesis were investigated *in vitro*. Then, osteoblastic differentiation capacity of SCAPs with RA-BMP-2 scaffolds was analyzed by ALP activity and expression of osteoblast-related genes.

Results: A porous nanofiber microstructure endowed this scaffold with the ability to maintain the survival of HUVECs and SCAPs. The RA-VEGF/BMP-2 drug delivery systems exhibited several advantages *in vitro*: injectability, biodegradability, good biocompatibility, and noncytotoxicity. Released rhVEGF$_{165}$/BMP-2 were proved to promote angiogenesis of HUVECs as well as osteogenesis of SCAPs abilities.

Conclusion: RATEA16 loading with VEGF and BMP-2 might be a potential clinical strategy for tissue engineering, especially in bone reconstruction, due to its ability of delivering growth factors effectively and efficiently.

KEYWORDS

angiogenesis, bone reconstruction, drug delivery system, osteogenesis, self-assembling peptide hydrogel, sustained release

1 | INTRODUCTION

Bone defect repair, a serious problem in clinical practice, occurs in cases of trauma, tumor resection, congenital malformations, infections, or reconstructive surgery (Majidinia et al., 2018; Xin et al., 2017). The current strategies for bone defects are nature bone grafting (autologous, allogeneic) and synthetic bone grafting (ceramics metals polymers and their combinations); however, shortages and complications of donor sites, graft rejection, and high expenditure limit their clinical applications. Bone is a highly vascularized tissue that relies on the close connection between blood vessels and bone cells to maintain skeletal integrity (Aryal et al., 2014; Garcia et al., 2016; Kanczler & Oreffo, 2008). Hence, bone reconstruction requires an efficient blood supply to deliver nutrients, oxygen, and cells to regenerating sites (Zigdon-Giladi et al., 2017). Unfortunately, current strategies for bone repair

Ruijuan Zhang and Yang Liu contributed equally to this work.

are limited by insufficient vascularization (Quinlan et al., 2017). To address this problem, bone tissue engineering, for instance, is expected to provide new therapeutic methods (Dou et al., 2019; Quinlan et al., 2015). Recognized strategies in bone tissue engineering combine three essential elements—scaffolds, stem cells, and growth factors—to produce a tissue-engineered system (Vieira et al., 2017). A variety of biomaterials, such as polymeric matrices (Taleb et al., 2019; J. Xu, Han, et al., 2019; Y. Xu, Han, et al., 2019), ceramic scaffolds (Diaz-Rodriguez et al., 2018) or hydrogel-based materials (Barati et al., 2016), encapsulating different functional factors to induce the formation of bone and blood vessels have been designed and optimized.

Hydrogels, a kind of viscoelastic material, hold promise in a number of complex applications, including drug delivery and tissue engineering (Qi et al., 2018; Zhao et al., 2008). One kind of hydrogel made from self-assembled peptides exhibits several advantages: a rational design, easy synthesis, forming hydrogels with various viscoelastic properties, injectability, biocompatibility, biodegradability, and the ability to incorporate different bioactive motifs or molecules (Cho et al., 2012; Zhou et al., 2016). For instance, a hydrogel self-assembled by oligopeptide RADA16 ([CH3CONH]RADARADARADARADA-[CONH2]) has been commercialized (Yokoi et al., 2005). However, to achieve its sol-gel transition, a complex procedure in which pH of its solution changes gradually from acidic to neutral by solvent substitution is required. Moreover, precipitation occurs when the hydrogel is stirred in a neutral environment (Zhao et al., 2008). To overcome these obstacles, we utilized the RATEA16 (RA, [CH3CONH]-RATARAEARATARAEA-[CONH2]) previously designed by our group in this study. This peptide consists of four cationic and two anionic residues, allowing it to establish a different self-organized structure at neutral pH, leading to spontaneous formation of stable and transparent hydrogels following a simple procedure without importing any external toxic initiator (Zhao et al., 2008). The hydrogels are constructed by interconnecting β-sheet nanofibers with extremely high water content (>99.5% [w/v]). Moreover, they could undergo pH-reversible transitions from viscous solution to elastic hydrogel and to precipitate, which can be used in controlled release of therapeutics (Zhao et al., 2008).

As an important morphogenic factor, bone morphogenetic protein 2 (BMP-2) has been shown to be odontogenic and osteogenic both *in vitro* and *in vivo* (W. Wang, Dang, et al., 2016). Similarly, the widely used vascular endothelial growth factor (VEGF) has routinely been delivered to increase vascularization *in vivo* by promoting early events in angiogenesis, particularly in vascular endothelial and epithelial cell proliferation and survival, vascular endothelial cell migration, and blood vessel formation (Adini et al., 2017; Ferrara, 2004; Senger DR & Peruzzi CA, 1996). However, the short half-life, high cost, need for repeated administration, high-cumulative dose, and toxicity to cells limit the direct injection of VEGF into a defect site (W. Wang, Dang, et al., 2016). Meanwhile, exposure to high-dose levels of BMP-2 may be sufficient to induce ectopic bone formation. High-dose BMP-2 treatment is also associated with increased inflammation, leading to the production of inflammatory cytokines, heterotopic ossification, and reduced bone quality. As the bioactivity of BMP-2 and VEGF is concentration- and time-dependent, their sustained delivery from biodegradable matrices is essential for bone regeneration but remains unfulfilled, therefore warranting an in-depth investigation (Barati et al., 2016).

Stem cells of the apical papilla (SCAPs) are a population of dental stem cells that have been shown to hold great potential in regenerative endodontics and bone formation (Ruparel et al., 2013). SCAPs exhibit multipotency of differentiating into osteogenic, angiogenic, and other lineages (Bakopoulou et al., 2011; Sonoyama et al., 2008). In addition, studies demonstrated that when SCAPs and scaffolds were subcutaneously implanted into immunocompromised mice, bone-like mineralized tissues were produced in situ ultimately (Abe et al., 2008; Kang et al., 2019). SCAPs are easily harvested from premolars or wisdom teeth extracted during orthodontic treatment, they appear to be a reliable source of stem cells for tissue engineering, particularly in bone regeneration (Yuan et al., 2015).

Herein, we utilized the RATEA16 hydrogel scaffold encapsulating rhVEGF$_{165}$ and BMP-2 to establish drug-loading hydrogel systems, then investigated their release patterns and functions through the vasculogenic/osteogenic differentiation of human HUVECs and SCAPs in vitro. This research aims to provide evidence demonstrating the injectable self-assembled RATEA16 hydrogel as an efficient drug delivery carrier that sustained release of VEGF and BMP-2 to promote vascular and bone formation. These systems may serve as options for bone regeneration with future clinical applications.

2 | MATERIALS AND METHODS

2.1 | Hydrogel formation and characterization

2.1.1 | Hydrogel formation

Lyophilized RATEA16 peptide (synthesized by Top-peptide Corporation, Shanghai, China) was dissolved in DMEM at a concentration of 5 mg/ml (wt/vol; 0.5%). The pH of the peptide solution was adjusted to neutral (~pH 7.4) using a pH 7.5 Tris·HCl buffer, at which point the peptide solution immediately adopted a hydrogel state.

2.1.2 | Scanning electron microscopy (SEM) analysis

The morphology of the hydrogel was observed using *SEM* (S-4800, Hitachi, Japan). The hydrogel was immersed in liquid nitrogen by the freeze-fracture method, freeze-dried, sliced, sputter coated with gold, and subjected to observation by *SEM*. To observe the microstructure

of cells encapsulated in the RATEA16 hydrogel, the gel was fixed in 2.5% glutaraldehyde for 2 hr immersed in 0.18 mol/L sucrose for 2 hr at 4°C, rehydrated in an ethanol series, and then subjected to the freeze-fracture method above. Image J software (1.48v, National Institutes of Health, USA) was used to analyze *SEM* images and calculate their porosity. Porosity (%) = (pore area ÷ total area) ×100%.

2.1.3 | *In vitro* degradation studies

Hydrogel samples were weighed and then immersed in distilled water (~pH 7.4) at room temperature for 30 days. The percent weight loss (% WL) of the hydrogel was determined during the incubation at specified time points. The following formula was used: % WL = [(Wi-Wf) / Wi] ×100%, where Wi and Wf are the weights of the hydrogel before and after incubation in distilled water, respectively.

2.1.4 | Formation of RA-VEGF/BMP-2 scaffolds and *in vitro* drug release assay

$rhVEGF_{165}$ and BMP-2 solutions were prepared by dissolving lyophilized $rhVEGF_{165}$ and BMP-2 powders, respectively, in a sterile PBS/HCL solution containing 0.1 wt% BSA. Then, these solutions were mixed with 200 μl of 0.5% RATEA16 peptide to form VEGF-loaded and BMP-2-loaded hydrogels, respectively, containing 100 ng of $rhVEGF_{165}$ and 300 ng of BMP-2, respectively, as described above. To further investigate the drug release characteristics of the RATEA16 hydrogel, 200 μl of RA-VEGF hydrogel or RA-BMP-2-loaded hydrogel was carefully transferred into 24-well Transwell inserts (Corning, USA) with 1 ml of distilled water in the lower chambers and then incubated at 37°C. Wells with chamber that were not filled with distilled water were used as controls. A total volume of 100 μl of the supernatant in each well were obtained after 1, 3, 6, 9, and 12 days, and the same volume of fresh distilled water was then added. Supernatant samples were stored in a − 80°C freezer, and the $rhVEGF_{165}$/BMP-2 protein concentrations were later measured by ELISA.

2.2 | Cell culture and cytotoxicity studies

2.2.1 | Cell culture

HUVECs were purchased from ScienCell Research Laboratories (San Diego, CA, USA) and cultured in ECM (ScienCell) containing 5% FBS (ScienCell), 1% endothelial cell growth supplement (ECGS, ScienCell), and 1% penicillin/streptomycin (P/S) (Invitrogen, Eugene, OR, USA). We obtained apical papilla from the extracted third molars of healthy patients (3 donors aged 8–17 years) required by orthodontic treatment. Then, SCAPs were isolated according to a published procedure and cultured in DMEM (Invitrogen) supplemented with 5% FBS and 1% P/S (Ruparel et al., 2013). All cells were maintained in humidified air with 5% CO_2 at 37°C and subcultured for between 3 and 6 generations for subsequent experiments. This study was approved by the Peking University of Stomatology of Hospital Ethics Committee.

2.2.2 | Cytotoxicity assay

To investigate the cytotoxicity of the RATEA16 hydrogel, extract liquid was collected after incubation in ECM or DMEM at 37°C for 72 hr and stored at − 20°C. HUVECs or SCAPs were seeded into 96-well plates at a density of 2×10^3 cells/well, starved with free-serum medium for 24 hr, and then incubated with extract liquid for 24 hr and 48 hr. A CCK-8 assay was carried out following the manufacturer's instructions, and the absorbance at a wavelength of 450 nm was measured using an automatic enzyme-linked immunosorbent assay reader (ELx800, BioTek Instruments, Inc., USA).

2.3 | Effects of RA-VEGF scaffolds on HUVECs angiogenesis

2.3.1 | Cell proliferation assay

In our preliminary experiments, the proliferation of HUEVCs in different concentrations of $rhVEGF_{165}$ was tested by CCK-8 assay, which revealed that 50ng/ml of $rhVEGF_{165}$ had the most significant effect (data not shown). Then, HUVECs were seeded into 24-well plates at a density of 6×10^3 cells/well and incubated under three conditions: RA-VEGF scaffolds loading in the upper chambers of Transwells, medium containing free $rhVEGF_{165}$ (50 ng/ml), and complete medium. The CCK-8 assay was performed at the expected time points (1 d, 3 d, 5 d, 7 d) as described by the method above.

2.3.2 | Determination of cell migration by wound healing assay

HUVECs were cultured in 6-well plates (5×10^5 cells/well) until they reached monolayer confluence and then scratched horizontally with a sterile pipette tip. The cells were then administrated of fresh medium containing 2% FBS with or without $rhVEGF_{165}$ (50 ng/ml), or RA-VEGF scaffolds for 24 hr. Five images of each well were taken, and the percentage of regeneration was analyzed with Wimasis website (https://www.wimasis.com/en/).

2.3.3 | Determination of cell migration by transwell assay

HUVECs were cultured in Transwell inserts (8 mm pore-size) at a density of 1×10^4 cells/well in 24-well plates, while RA-VEGF scaffolds and ECM were placed in the bottom chambers. After 6 hr of incubation, non-migrated cells in the upper chambers were removed, and the remaining cells were fixed and successively stained with 0.5% crystal violet for

TABLE 1 Sequences of primers used for real-time RT-PCR

Gene	Forward primer	Reverse primer
GAPDH	CGACAGTCAGCCGCATCTT	CCAATACGACCAAATCCGTTG
ALP	GACCTCCTCGGAAGACACTC	TGAAGGGCTTCTTGTCTGTG
OSX	CCTCCTCAGCTCACCTTCTC	GTTGGGAGCCCAAATAGAAA
OCN	AGCAAAGGTGCAGCCTTTGT	GCGCCTGGGTCTCTTCACT
OPN	ATGATGGCCGAGGTGATAGT	ACCATTCAACTCCTCGCTTT
Col Ia1	GAGGGCCAAGACGAAGACATC	CAGATCACGTCATCGCACAAC

30 min. To quantify the cells passed through the porous membrane, images were captured with an inverted phase-contrast microscope. Four fields of each well were then selected randomly for cell counting.

2.3.4 | Tube formation assay

After thawing on ice overnight, 200 μl/well of growth factor-reduced Matrigel was added to prechilled 24-well plates and polymerized for 1 hr at 37°C. Then, HUVECs (9×10^4 cells/well) were seeded onto the Matrigel layer, followed by starvation in medium containing half volume of serum without ECGS overnight. Once HUVECs had attached, chambers coated with RA-VEGF scaffolds were inserted into wells, while medium containing free 50 ng/ml $rhVEGF_{165}$ was added to wells used as the control group. After 24 hr and 72 hr of incubation, tube formation was observed and captured using an inverted phase-contrast microscope. The total branching length of the tubules was analyzed with ImageJ software.

2.4 | Effects of RA-BMP-2 scaffolds on SCAPs osteogenesis

Different concentrations of BMP-2 were first administrated to SCAPs to verify their osteoinductive ability by testing ALP activity and osteogenic-related gene expression. We final selected BMP-2 of 100 ng/ml for the working concentration as it promoted osteogenic differentiation of SCAPs mostly (data not shown). Human SCAPs were then seeded into 12-well plates at a density of 4×10^4 cells/well. When the cells reached 80% confluence, RA-BMP-2 scaffolds were placed into inserts, while complete medium or complete medium with free BMP-2 (100 ng/ml) in the lower chambers without insert were used as a negative or positive control group, respectively. The medium was changed every third day, and cells were cultured for 7 and 14 days.

2.4.1 | Alkaline phosphatase (ALP) staining and ALP activity assay

SCAPs were fixed with 4% paraformaldehyde and then processed with an ALP histochemical staining kit (Beyotime, Shanghai, China). The images were obtained with a scanner (HP, CA, USA). To further evaluate ALP activity, an ALP activity assay kit (Beyotime, Shanghai, China) was used. The absorbance of the solution at 520 nm was determined with a spectrophotometer (PerkinElmer, Waltham Mass, MA), while the total protein was measured with a BCA kit (Thermo Fisher Scientific, Waltham, MA) and used to normalize ALP activity.

2.4.2 | Real-time reverse transcriptase PCR (real-time RT-PCR)

Total RNA was extracted using TRIzol reagent (Invitrogen) and reverse transcribed into cDNA with 5 × PrimeScript RT Master Mix (TaKaRa). Real-time PCR was performed with a SYBR Green PCR kit (Roche Applied Science, IN, USA) on an ABI 7,500 Real-time PCR System (Applied Biosystems, CA, USA) to determine the mRNA expression levels of alkaline phosphatase (*ALP*), osteopontin (*OPN*), osteocalcin (*OCN*), collagen I (*Col I*), osterix (*OSX*), and *GAPDH*. The primers sequences were based on our previously published paper (Liu et al., 2019) Relative gene expression levels were calculated using the $2^{-\Delta\Delta CT}$ method and normalized to the mRNA level of *GAPDH*. Primer sequences are listed in Table 1.

2.5 | Statistical analysis

All experiments were repeated three times independently, and the results are presented as the means ± SD. Data represent the average of three independent experiments. Differences among groups were assessed by one-way analysis of variance (ANOVA) and Tukey's post hoc test. Differences with a P-value < 0.05 were considered statistically significant.

3 | RESULTS

3.1 | Characterization of the RATEA16 (RA) hydrogel

When a neutral pH was reached, the dissolving RATEA16 peptide immediately achieved sol-gel transition. Hydrogel formed under this process was defined as self-supporting since it was possible to invert the container without any collapse (Figure 1a). Our observation that this hydrogel could be injected through a needle attached to a syringe demonstrated its injectable property (Figure 1b). The RATEA16 hydrogel presented a porous microstructure with the porosity of (67.3 ± 9.4)

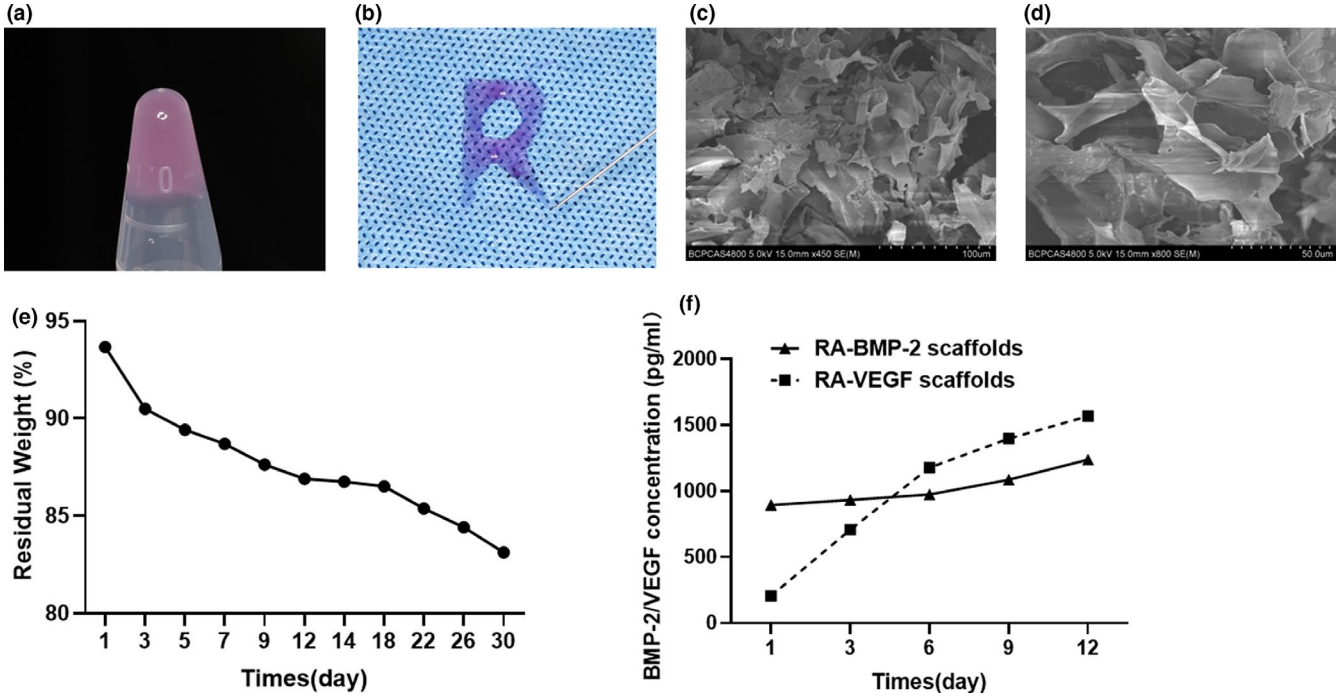

FIGURE 1 (a) The RATEA16 hydrogel (0.5% [wt/vol]) formed completely at pH 7.4. (b) Exhibition showing that the RATEA16 hydrogel could be injected through a syringe. *SEM* of RATEA16 scaffolds at a 0.5% (wt/vol) concentration at low magnification (c) (scale bar, 100 μm) and high magnification (d) (scale bar, 50 μm). (e) Curve showing degradation of the RATEA16 hydrogel within 30 days. (f) Graph showing the kinetics of BMP-2/VEGF release from the scaffold. The results are expressed as the mean ± *SD*

% and interconnected interior structure in *SEM* micrographs (Figure 1c and 1d). The degradation ability of the hydrogel was further tested. 10% of the hydrogel dissolved for the first 3-day period, following which its degradation rate remained slow, and the hydrogel exhibited an 83.13% residual weight at the end of a 1-month duration (Figure 1e).

3.2 | Kinetics of rhVEGF$_{165}$/BMP-2 release from the scaffolds

The Kinetics of released rhVEGF$_{165}$/BMP-2 from the scaffolds were measured by the weighting mode and the release curves were presented in Figure 1f, respectively. The burst release of VEGF was clearly observed over the first 6 days, following which the rate of release gradually decreased. Finally, a total of 1.6% of the VEGF were released from the scaffold over 12 days. By contrast, the release of BMP-2 from the RA-BMP-2 scaffolds was slow over the first 6 days but then gradually increased. At the end of 12 days, 0.4% of the loaded BMP-2 had been released. These results revealed that a low but sustained dose of VEGF/BMP-2 could be released from the scaffolds.

3.3 | Survival of HUVECs and SCAPs encapsulated in the RATEA16 hydrogel

To detect the cytotoxicity of the hydrogel, HUVECs and SCAPs were cultured in the supernatant of the RATEA16 hydrogel for 24 hr and 48 hr and evaluated by CCK-8 assay. Cell viability was slightly enhanced by 10%-12% in hydrogel supernatant comparing with those in complete culture medium (ECM for HUVECs and DMEM for SCAPs) without significant difference (Figure 2a and 2b). Cells were then implanted in the RATEA16 hydrogel and cultured for 3 days to explore the potential utilization of the hydrogel as a biomimetic scaffold for cell growth, proliferation, and differentiation. As shown in Figure 2c, HUVECs and SCAPs in this hydrogel appeared round shape and were evenly distributed in the gel under an inverted phase-contrast microscope, meanwhile presented great cell viability under *SEM* observation. Furthermore, cells cultured in the RATEA16 hydrogel proliferated efficiently within 14 days (Figure 2d).

3.4 | Effects of RA-VEGF scaffolds on proliferation, migration, and vascularization of HUVECs

3.4.1 | rhVEGF$_{165}$ released from RA-VEGF scaffolds promoted proliferation of HUVECs

We further applied cell proliferation assay to confirm that the release of VEGF from RA-VEGF scaffolds could maintain an efficient dose throughout to promote HUVECs proliferation. As shown in Figure 3a, HUVECs cultured with RA-VEGF scaffolds displayed 1.4-fold enhancement of cell growth compared to cells cultured in the absence of VEGF, which was even greater than VEGF (50 ng/ml) added directly to the medium.

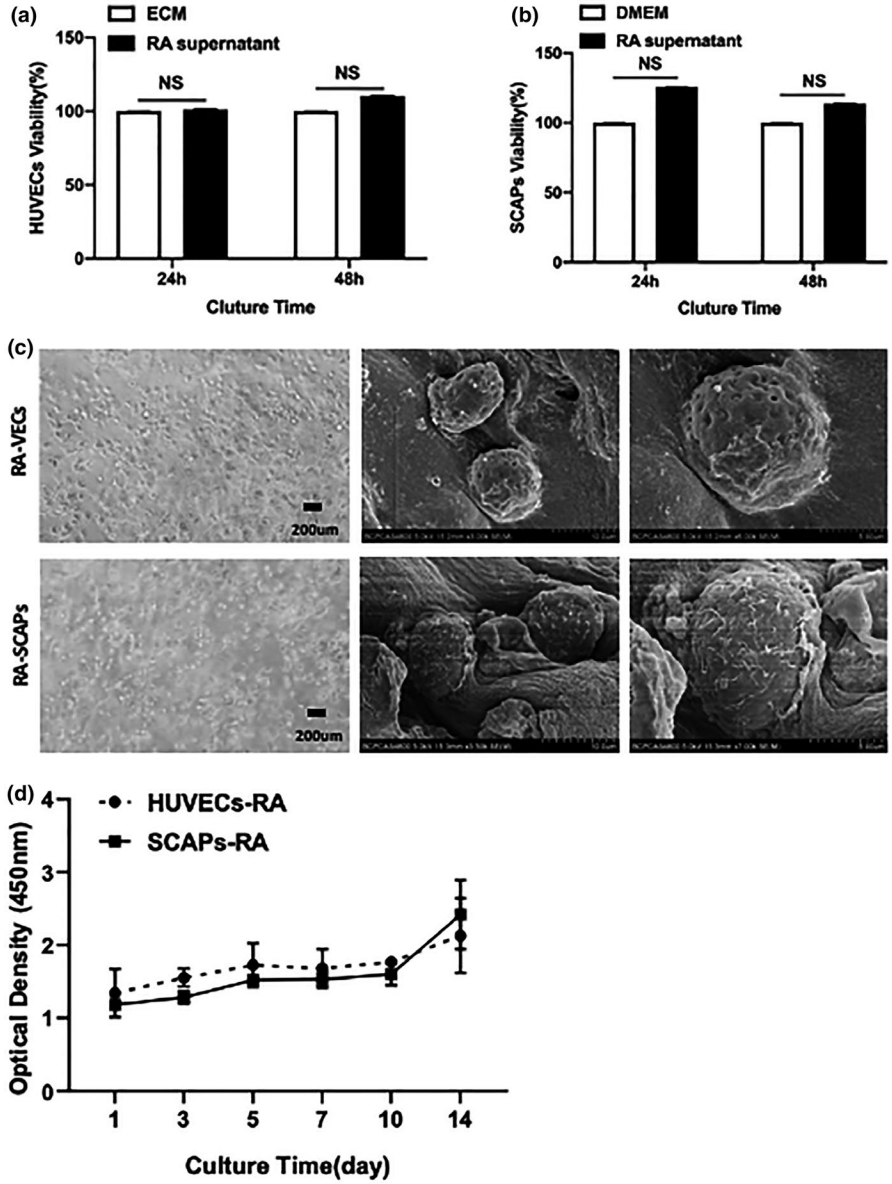

FIGURE 2 CCK-8 assays demonstrated that the RATEA16 hydrogel was not cytotoxic in HUVECs (a) and SCAPs (b). (c) Photograph of HUVECs/SCAPs encapsulated in the RATEA16 hydrogel by inverted microscopy (scale bar, 200 μm) and *SEM* (scale bars, 10 μm and 5 μm). (d) Proliferation of HUVECs and SCAPs in the RATEA16 hydrogel over 2 weeks. The results are expressed as the mean ± *SD* (n.s., $p > .05$.)

3.4.2 | rhVEGF$_{165}$ released from RA-VEGF scaffolds enhanced the migration of HUVECs

Migration is an essential procedure in the angiogenic process. We employed two methods to verify the migration of HUVECs under the treatment of RA-VEGF hydrogel. The scratch assay showed that free rhVEGF$_{165}$ enhanced cell migration by 4.5-fold compared with that in the control group. Encouragingly, cell migration in RA-VEGF scaffolds treated group exhibited 1.3-fold increase than that in free rhVEGF$_{165}$ group (Figure 3b and 3c). In addition, Transwell assay was performed to further measure the influence of VEGF released from the scaffolds on HUVECs migration. A clear promotion of cell migration was observed in free rhVEGF$_{165}$-treated HUVECs. HUVECs migrated more active under the stimulation of VEGF released from the scaffolds by 12-fold when comparing with those incubated in medium without VEGF administration, and by 1.3-fold when compared with those incubated in medium enriched with free VEGF, indicating a greater capability of RA-VEGF scaffold to cell migration improvement than that of free VEGF (Figure 3d and 3e).

3.4.3 | Effect of RA-VEGF scaffolds on tube formation

Cell tubule formation assay was applied to verify the angiogenesis of HUVEC. As shown in Figure 4a, VEGF released from the scaffolds increased tubule formation of HUVEs compared to cells cultured without VEGF for 12 hr, which exhibited similar effect with free rhVEGF$_{165}$ enriched medium. Surprisingly, the tubules in free rhVEGF$_{165}$ treatment appeared to be decomposed at 72 hr, while the cells incubated with RA-VEGF scaffolds still displayed intact tubules at that moment. These manifestations indicated that the sustained and low-dose release of VEGF from RA-VEGF scaffolds could promote tube formation continuously (Figure 4b).

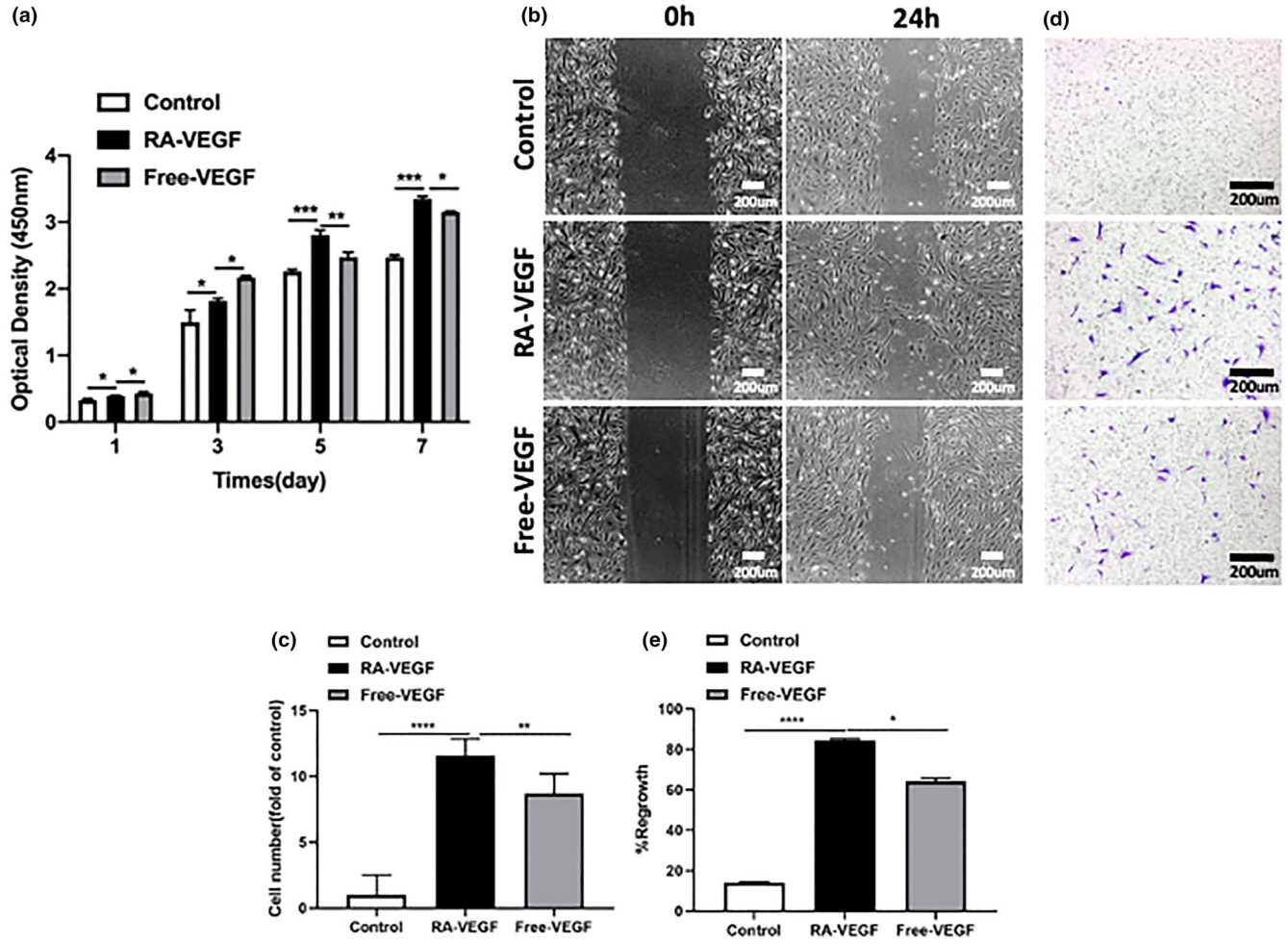

FIGURE 3 (a) Effect of VEGF released from RA-VEGF scaffolds on HUVEC proliferation. (b) Influence of VEGF released from RA-VEGF scaffolds on HUVEC migration determined by scratch assay. Scale bar, 200 μm. (c) Quantification of HUVEC migration by scratch assay. The results are expressed as the mean ± *SD* (**** $p < .0001$; ** $p < .01$). (d) Influence of VEGF released from RA-VEGF scaffolds on HUVEC migration determined by Transwell assay. Scale bar, 200 μm. (e) Quantification of HUVEC migration by Transwell assay. The results are expressed as the mean ± *SD* (**** $p < .0001$; * $p < .05$)

3.5 | Stimulation of osteogenic differentiation by RA-BMP-2 scaffolds

The function of BMP-2 released from RA-BMP-2 scaffolds in the osteogenic differentiation of SCAPs was investigated. ALP staining showed that ALP expression was significantly increased in free BMP-2 group and RA-BMP-2 group. ALP activity assays further confirmed those results by showing higher ALP activity in RA-BMP-2 scaffolds group compared with control group at 7 and 14 days (1.6-fold and 3.3-fold), respectively, while it was lower than in free BMP-2 group (Figure 5a and 5b).

Real-time RT-qPCR analysis demonstrated that the expression of *ALP*, *OPN*, *OCN*, and *Col I* in RA-BMP-2 scaffolds treated group increased by 1.5–3 folds compared with their expression in the control group at 7 and 14 days; meanwhile, the expression of *OSX* was enhance by 85-fold and 230-fold at 7 and 14 days, respectively ($p < .05$, Figure 5c). Interestingly, at 14 days, *OCN* was even more highly expressed in the group incubated with RA-BMP-2 scaffold than in the group incubated with free BMP-2 ($p < .05$), while *ALP* and *OSX* expression were lower. As contrast, *Col I* and *OCN* expression levels at 7 days as well as *Col I* expression levels at 14 days were not significantly different between the groups (Figure 5c).

4 | DISCUSSION

The reconstruction of bone defects due to infection, trauma, tumor, heredity, periodontal disease, anatomical, or congenital abnormalities remains a major clinical issue for oral surgeons. Scaffolds have played a crucial role as supporting materials for various cell growth processes and gradually evolved into bioactive matrices that also supply pro-regenerative factors to enhance tissue regeneration (Quinlan et al., 2017). The short self-assemble peptide RATEA16 with high water content, network nanostructure, ability to recover from mechanical breakdowns has been designed by our group previously (Zhao et al., 2008). The hydrogel also can be used in controlled

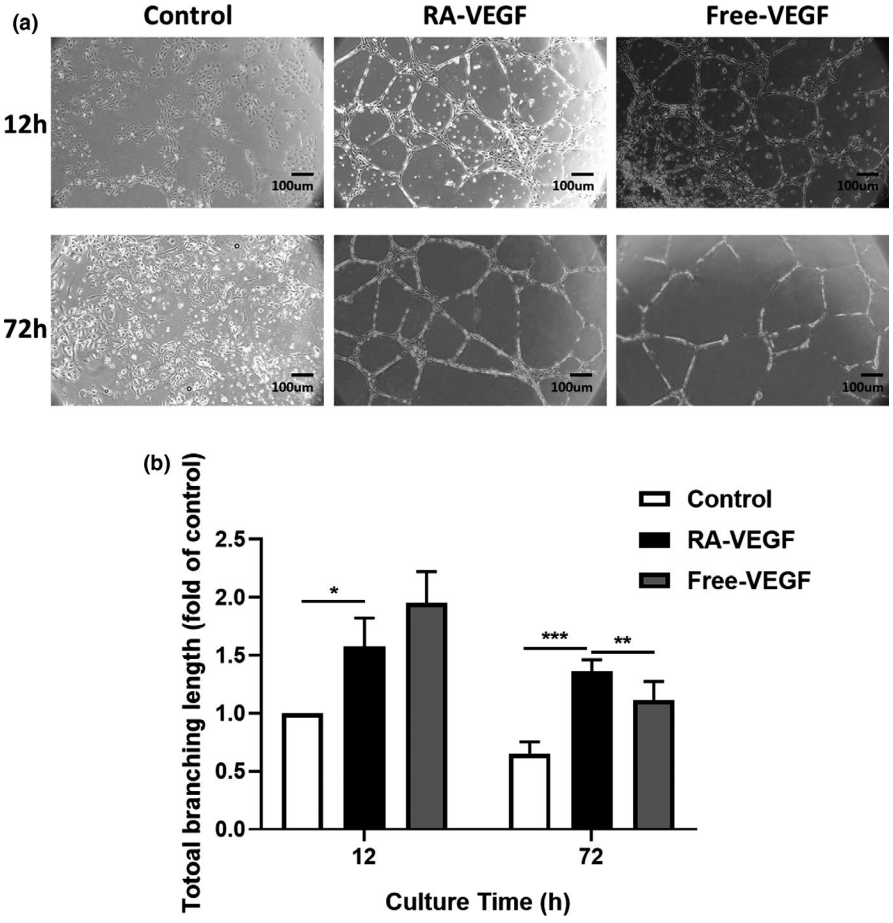

FIGURE 4 Effects of VEGF released from RA-VEGF scaffolds on tube formation in HUVECs. (a) Images showing tube formation after 12 and 72 hr of culture under a phase-contrast microscope. Scale bar, 100 μm. (The images are representative experiments.) (b) Quantification of tube formation. The results are expressed as the mean ± *SD* (*** $p < .001$; * $p < .05$)

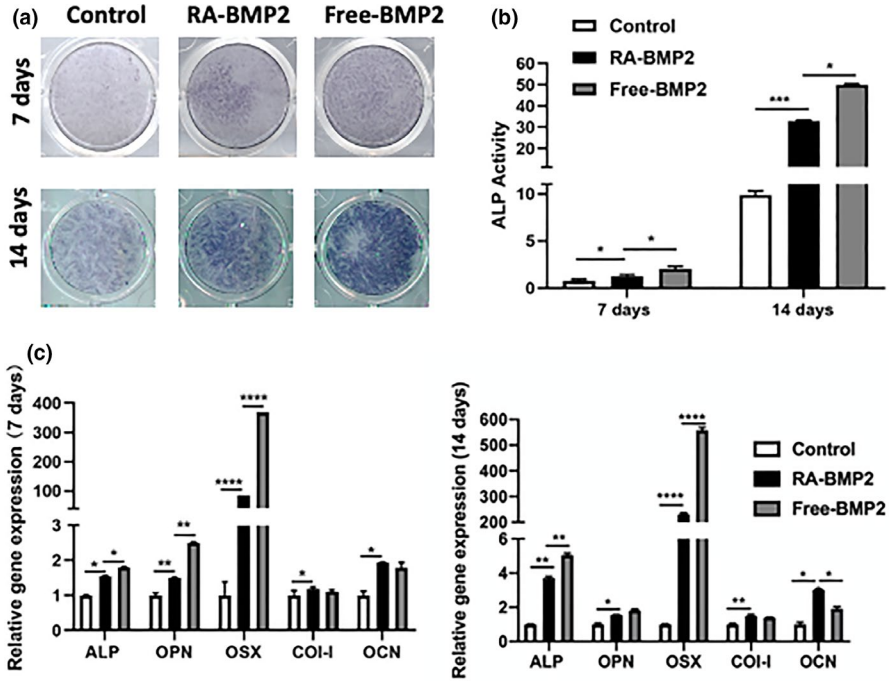

FIGURE 5 Influence of BMP-2 released from the RA-BMP-2 scaffold on ALP activity and the expression of osteoblast-associated genes in SCAPs. (a) ALP staining of SCAPs after induction with RA-BMP-2 scaffold for 7 days or 14 days. (b) Analysis of ALP activity in SCAPs after incubation with RA-BMP-2 scaffold for 7 days or 14 days. The results are expressed as the mean ± *SD* (*** $p < .001$; * $p < .05$). (c) Quantitative determination of the mRNA levels of ALP, OPN, OSX, COI-I, and OCN in SCAPs after induction with RA-BMP-2, free BMP-2 or proliferation medium for 7 days or 14 days. The results are expressed as the mean ± *SD* (**** $p < .0001$; ** $p < .01$; * $p < .05$)

release of therapeutics through pH-response and in diffusion release. The aim of our study was to establish a sustained release drug delivery system with the RATEA16 hydrogel that could release bioactive agents in a slow and continuous manner while maintaining their biological effects. The results demonstrated that the RA-VEGF/BMP-2 scaffolds underwent a rapid self-assembly process, exhibited nanofibers microstructures, benefited for cell survive and proliferation, and facilitated the sustained release of $rhVEGF_{165}$ and

BMP-2, which increased the angiogenesis of HUVECs and the osteogenic differentiation of SCAPs. This RATEA16 hydrogel-based drug delivery system would be a favorable system for bone regeneration.

An injectable hydrogel system is an appealing option for use in bony defects because it can be gelatinated in situ and effectively enter difficult sites of injury as a less invasive procedure, and then form a composite irrespective of shape and defect geometry. As a result, the treatment expenditure of surgery for patients could be reduced (Kondiah et al., 2016; C. Wang, Dang, et al., 2016). Interestingly, RATEA16 scaffolds possess the advantage of being injectable as they could feasibly be injected through a needle into a target location. As it exhibits rapid, simple self-assembly in a neutral environment and viscoelastic properties, the RATEA16 hydrogel selected for this study would be a candidate material for future clinical applications in the field of orthopedic science or even regenerative endodontics, in which tissue engineering procedures are limited in narrow and solid root canals.

To enhance the osteoinductivity of scaffolds for bone regeneration, several studies have applied delicate techniques to impregnate materials containing various growth factors, such as bone morphogenetic proteins (BMPs), VEGF, and fibroblast growth factors (FGFs) (Li et al., 2016). Nevertheless, current growth factor delivery approaches for VEGF and BMP-2 frequently exhibited unsuccessful delivery due to the uncontrolled release, potential cytotoxicity, and excessively expenditure (Quinlan et al., 2017). Previous studies have also shown that free VEGF has a relatively short half-life of 33.7 ± 13 min (Eppler et al., 2002), its burst release at high concentrations may induce the generation of hemangiomas and malformed vessels (Ozawa et al., 2004). In contrast, the slow and steady release of VEGF seems to be a preferable strategy. In our study, with the characterization of slow biodegrading, $rhVEGF_{165}$ was released from the RA-VEGF scaffolds in a relatively consistent way at an extraordinary low dose. To detect the bioactive activity of the released VEGF, a RA-VEGF scaffold containing the same amount of $rhVEGF_{165}$ in the positive control group (incubation with free $rhVEGF_{165}$) was designed. $rhVEGF_{165}$ released from the RA-VEGF scaffolds retained its biological activity, which manifested as the successfully inducing cell proliferation and migration in the horizontal and vertical directions of HUVECs. Moreover, tube formation assays revealed that $rhVEGF_{165}$ delivered from the RA-VEGF scaffolds had an even longer and stronger angiogenesis effect than free VEGF-treated group.

The RA-BMP-2 scaffolds we established displayed a drug release pattern analogous with that of the RA-VEGF system. These results suggested that even a small amount of BMP-2 released into the medium could still exhibit biological activity to promote osteogenesis differentiation. The expression of osteoblast-specific genes was significantly induced by BMP-2 released from scaffolds, for example, the level of *OCN* expression under this treatment was even higher than that in the free BMP-2-induced group.

The RATEA16 scaffolds developed in our group combined a highly porous nanofiber structure with properties specifically optimized to promote cell infiltration and proliferation. HUVECs and SCAPs implanted in the RATEA16 hydrogels were present as spheroids and exhibited steady cell proliferation. A spherical cellular morphology was proved to lead to advanced cell-to-cell contacts and cell-matrix interactions, which were more resistant to a hypoxic environment, inhibited apoptosis (Bhang et al., 2011, 2012), and enhanced the production of various growth factors (Lars Gaedtke et al., 2007).

The injectable scaffolds described herein represented a promising approach for overcoming the shortages of traditional hydrogel utilized bone defects repairing. The RA-VEGF/BMP-2 scaffolds could be synthesized easily and formed spontaneously in 5 min without importing any external toxic initiator. VEGF released from RA-VEGF scaffolds displayed enhanced capillary-like tube formation, similarly with free VEGF group, and even exhibited better on prolonging the regression of tubules which was normally observed between 12 and 24 hr as previously reported (McCoy et al., 2013). Meanwhile, the release of VEGF/BMP-2 from the scaffolds presented a continuous low-dose manner, which could reduce total dose of drug intake comparing to a single or serial local administration, and thus lower the risks of side effects caused by irritation from high drug concentration. Therefore, the RATEA 16 hydrogel has great potential in bone engineering, not only because it could be a drug delivery carrier for different growth factors, but also it may be used as a scaffold in engineering vascularized bone. In addition, this injectable RATAE16 hydrogel would be easily applied into certain narrow tissues, such as periodontal intrabony defects and periapical lesions. To further confirm the in vivo properties of this approach, animal models will have to be further implemented.

5 | CONCLUSION

All in all, this study demonstrated the injectable hydrogel RATEA16 into RA-VEGF/BMP-2 scaffolds that facilitate the sustained release of growth factors. This hydrogel showed superiority with features of easy synthesis and achieving sol-gel transition in normal physiological environment. It is also characterized by biodegradability, injectability, and biocompatibility. Cells implanted in the hydrogel exhibited round shape and continuous proliferation over time. Meanwhile, the bioactivity of released VEGF and BMP-2 was maintained, leading to enhanced cell proliferation, migration, and tube formation of HUVECs as well as cell osteogenesis of SCAPs. Furthermore, these hydrogel-based drug delivery systems serving as a potential approach in tissue engineering, especially in bone regeneration, need to test *in vivo* in future research.

ACKNOWLEDGEMENTS

The work was supported by the Peking University School and Hospital of Stomatology Science Foundation for Young Scientists [PKUSS20170106].

CONFLICT OF INTERESTS

The authors declare no conflict of interest.

AUTHOR CONTRIBUTIONS

Ruijuan Zhang : Conceptualization; Data curation; Formal analysis; Investigation; Methodology; Software; Writing-original draft; Writing-review & editing. **Yang Liu:** Conceptualization; Formal analysis; Investigation; Methodology; Software; Visualization. **Yingqiu Qi :** Conceptualization; Methodology; Software. **Ying Zhao :** Formal analysis; Resources; Validation. **Guangjun Nie :** Conceptualization; Resources; Validation; Visualization. **Xiaozhe Wang:** Conceptualization; Formal analysis; Funding acquisition; Project administration; Resources; Supervision; Writing-original draft; Writing-review & editing. **Shuguo Zheng:** Conceptualization; Funding acquisition; Project administration; Resources; Supervision; Validation; Visualization; Writing-review & editing.

PEER REVIEW

The peer review history for this article is available at https://publons.com/publon/10.1111/odi.13785.

ORCID

Ruijuan Zhang https://orcid.org/0000-0002-8719-3241
Yang Liu https://orcid.org/0000-0003-2359-6583
Xiaozhe Wang https://orcid.org/0000-0003-3312-6737
Shuguo Zheng https://orcid.org/0000-0001-6717-5196

REFERENCES

Abe, S., Yamaguchi, S., Watanabe, A., Hamada, K., & Amagasa, T. (2008). Hard tissue regeneration capacity of apical pulp derived cells (APDCs) from human tooth with immature apex. *Biochemical and Biophysical Research Communications*, *371*(1), 90–93. https://doi.org/10.1016/j.bbrc.2008.04.016

Adini, A., Adini, I., Chi, Z. L., Derda, R., Birsner, A. E., Matthews, B. D., & D'Amato, R. J. (2017). A novel strategy to enhance angiogenesis in vivo using the small VEGF-binding peptide PR1P. *Angiogenesis*, *20*(3), 399–408. https://doi.org/10.1007/s10456-017-9556-7

Aryal, R., Chen, X. P., Fang, C., & Hu, Y. C. (2014). Bone morphogenetic protein-2 and vascular endothelial growth factor in bone tissue regeneration: New insight and perspectives. *Orthop Surg*, *6*(3), 171–178. https://doi.org/10.1111/os.12112

Bakopoulou, A., Leyhausen, G., Volk, J., Tsiftsoglou, A., Garefis, P., Koidis, P., & Geurtsen, W. (2011). Comparative analysis of in vitro osteo/odontogenic differentiation potential of human dental pulp stem cells (DPSCs) and stem cells from the apical papilla (SCAP). *Archives of Oral Biology*, *56*(7), 709–721. https://doi.org/10.1016/j.archoralbio.2010.12.008

Barati, D., Shariati, S. R. P., Moeinzadeh, S., Melero-Martin, J. M., Khademhosseini, A., & Jabbari, E. (2016). Spatiotemporal release of BMP-2 and VEGF enhances osteogenic and vasculogenic differentiation of human mesenchymal stem cells and endothelial colony-forming cells co-encapsulated in a patterned hydrogel. *J Control Release*, *223*, 126–136. https://doi.org/10.1016/j.jconrel.2015.12.031

Bhang, S. H., Cho, S.-W., La, W.-G., Lee, T.-J., Yang, H. S., Sun, A.-Y., Baek, S.-H., Rhie, J.-W., & Kim, B.-S. (2011). Angiogenesis in ischemic tissue produced by spheroid grafting of human adipose-derived stromal cells. *Biomaterials*, *32*(11), 2734–2747. https://doi.org/10.1016/j.biomaterials.2010.12.035

Bhang, S. H., Lee, S., Shin, J. Y., Lee, T. J., & Kim, B. S. (2012). Transplantation of cord blood mesenchymal stem cells as spheroids enhances vascularization. *Tissue Engineering Part A*, *18*(19–20), 2138–2147. https://doi.org/10.1089/ten.TEA.2011.0640

Cho, H., Balaji, S., Sheikh, A. Q., Hurley, J. R., Tian, Y. F., Collier, J. H., Crombleholme, T. M., & Narmoneva, D. A. (2012). Regulation of endothelial cell activation and angiogenesis by injectable peptide nanofibers. *Acta Biomaterialia*, *8*(1), 154–164. https://doi.org/10.1016/j.actbio.2011.08.029

Diaz-Rodriguez, P., Sanchez, M., & Landin, M. (2018). Drug-loaded biomimetic ceramics for tissue engineering. *Pharmaceutics*, *10*(4), https://doi.org/10.3390/pharmaceutics10040272

Dou, D. D., Zhou, G., Liu, H. W., Zhang, J., Liu, M. L., Xiao, X. F., Fei, J. J., Guan, X. L., & Fan, Y. B. (2019). Sequential releasing of VEGF and BMP-2 in hydroxyapatite collagen scaffolds for bone tissue engineering: Design and characterization. *International Journal of Biological Macromolecules*, *123*, 622–628. https://doi.org/10.1016/j.ijbiomac.2018.11.099

Eppler, S. M., Combs, D. L., Henry, T. D., Lopez, J. J., Ellis, S. G., Yi, J.-H., Annex, B. H., McCluskey, E. R., & Zioncheck, T. F. (2002). A target-mediated model to describe the pharmacokinetics and hemodynamic effects of recombinant human vascular endothelial growth factor in humans*. *Clinical Pharmacology & Therapeutics*, *72*(1), 20–32. https://doi.org/10.1067/mcp.2002.126179

Ferrara, N. (2004). Vascular endothelial growth factor: Basic science and clinical progress. *Endocrine Reviews*, *25*(4), 581–611. https://doi.org/10.1210/er.2003-0027

Gaedtke, L., Thoenes, L., Culmsee, C., Mayer, B., & Wagner, E. (2007). Proteomic analysis reveals differences in protein expression in spheroid versus monolayer cultures of low-passage colon carcinoma cells. *Journal of Proteome Research*, *6*(11), 4111–4118. https://doi.org/10.1021/pr0700596

Garcia, J. R., Clark, A. Y., & Garcia, A. J. (2016). Integrin-specific hydrogels functionalized with VEGF for vascularization and bone regeneration of critical-size bone defects. *J Biomed Mater Res A*, *104*(4), 889–900. https://doi.org/10.1002/jbm.a.35626

Kanczler, J. M., & Oreffo, R. O. (2008). Osteogenesis and angiogenesis: The potential for engineering bone. *Eur Cell Mater*, *15*, 100–114. https://doi.org/10.22203/ecm.v015a08

Kang, J., Fan, W., Deng, Q., He, H., & Huang, F. (2019). Stem cells from the apical papilla: A promising source for stem cell-based therapy. *BioMed Research International*, *2019*, 6104738. https://doi.org/10.1155/2019/6104738

Kondiah, P. J., Choonara, Y. E., Kondiah, P. P., Marimuthu, T., Kumar, P., du Toit, L. C., & Pillay, V. (2016). A review of injectable polymeric hydrogel systems for application in bone tissue engineering. *Molecules*, *21*(11), https://doi.org/10.3390/molecules21111580

Li, J., Xu, Q., Teng, B., Yu, C., Li, J., Song, L., Lai, Y.-X., Zhang, J., Zheng, W., & Ren, P.-G. (2016). Investigation of angiogenesis in bioactive 3-dimensional poly(d, l-lactide-co-glycolide)/nano-hydroxyapatite scaffolds by in vivo multiphoton microscopy in murine calvarial critical bone defect. *Acta Biomaterialia*, *42*, 389–399. https://doi.org/10.1016/j.actbio.2016.06.024

Liu, Y., Sun, X., Zhang, X., Wang, X., Zhang, C., & Zheng, S. (2019). RUNX2 mutation impairs osteogenic differentiation of dental follicle cells. *Archives of Oral Biology*, *97*, 156–164. https://doi.org/10.1016/j.archoralbio.2018.10.029

Majidinia, M., Sadeghpour, A., & Yousefi, B. (2018). The roles of signaling pathways in bone repair and regeneration. *Journal of Cellular Physiology*, *233*(4), 2937–2948. https://doi.org/10.1002/jcp.26042

McCoy, R. J., Widaa, A., Watters, K. M., Wuerstle, M., Stallings, R. L., Duffy, G. P., & O'Brien, F. J. (2013). Orchestrating osteogenic differentiation of mesenchymal stem cells–identification of placental growth factor as a mechanosensitive gene with a pro-osteogenic role. *Stem Cells*, *31*(11), 2420–2431. https://doi.org/10.1002/stem.1482

Ozawa, C. R., Banfi, A., Glazer, N. L., Thurston, G., Springer, M. L., Kraft, P. E., McDonald, D. M., & Blau, H. M. (2004). Microenvironmental VEGF concentration, not total dose, determines a threshold between normal and aberrant angiogenesis. *J Clin Invest*, *113*(4), 516–527. https://doi.org/10.1172/JCI18420

Qi, Y., Min, H., Mujeeb, A., Zhang, Y., Han, X., Zhao, X., Anderson, G. J., Zhao, Y., & Nie, G. (2018). Injectable hexapeptide hydrogel for localized chemotherapy prevents breast cancer recurrence. *ACS Applied Materials & Interfaces*, *10*(8), 6972–6981. https://doi.org/10.1021/acsami.7b19258

Quinlan, E., Lopez-Noriega, A., Thompson, E. M., Hibbitts, A., Cryan, S. A., & O'Brien, F. J. (2017). Controlled release of vascular endothelial growth factor from spray-dried alginate microparticles in collagen-hydroxyapatite scaffolds for promoting vascularization and bone repair. *J Tissue Eng Regen Med*, *11*(4), 1097–1109. https://doi.org/10.1002/term.2013

Quinlan, E., Partap, S., Azevedo, M. M., Jell, G., Stevens, M. M., & O'Brien, F. J. (2015). Hypoxia-mimicking bioactive glass/collagen glycosaminoglycan composite scaffolds to enhance angiogenesis and bone repair. *Biomaterials*, *52*, 358–366. https://doi.org/10.1016/j.biomaterials.2015.02.006

Ruparel, N. B., de Almeida, J. F., Henry, M. A., & Diogenes, A. (2013). Characterization of a stem cell of apical papilla cell line: Effect of passage on cellular phenotype. *J Endod*, *39*(3), 357–363. https://doi.org/10.1016/j.joen.2012.10.027

Senger, D. R., Ledbetter, S. R., Claffey, K. P., Papadopoulos-Sergiou, A., Peruzzi, C. A., & Detmar, M. (1996). Stimulation of endothelial cell migration by vascular permeability factor_vascular endothelial growth factor through cooperative mechanisms involving the abf3 integrin, osteopontin. *The American Journal of Pathology*, *149*(1), 293–305.

Sonoyama, W., Liu, Y., Yamaza, T., Tuan, R. S., Wang, S., Shi, S., & Huang, G. T. (2008). Characterization of the apical papilla and its residing stem cells from human immature permanent teeth: A pilot study. *J Endod*, *34*(2), 166–171. https://doi.org/10.1016/j.joen.2007.11.021

Taleb, M., Ding, Y., Wang, B., Yang, N. A., Han, X., Du, C., Qi, Y., Zhang, Y., Sabet, Z. F., Alanagh, H. R., Mujeeb, A., Khajeh, K., & Nie, G. (2019). Dopamine delivery via pH-Sensitive nanoparticles for tumor blood vessel normalization and an improved effect of cancer chemotherapeutic drugs. *Adv Healthc Mater*, *8*(18), e1900283. https://doi.org/10.1002/adhm.201900283

Vieira, S., Vial, S., Reis, R. L., & Oliveira, J. M. (2017). Nanoparticles for bone tissue engineering. *Biotechnology Progress*, *33*(3), 590. https://doi.org/10.1002/btpr.2469

Wang, C., Wang, X., Dong, K., Luo, J., Zhang, Q., & Cheng, Y. (2016). Injectable and responsively degradable hydrogel for personalized photothermal therapy. *Biomaterials*, *104*, 129–137. https://doi.org/10.1016/j.biomaterials.2016.07.013

Wang, W., Dang, M., Zhang, Z., Hu, J., Eyster, T. W., Ni, L., & Ma, P. X. (2016). Dentin regeneration by stem cells of apical papilla on injectable nanofibrous microspheres and stimulated by controlled BMP-2 release. *Acta Biomaterialia*, *36*, 63–72. https://doi.org/10.1016/j.actbio.2016.03.015

Xin, T., Gu, Y., Cheng, R., Tang, J., Sun, Z., Cui, W., & Chen, L. (2017). Inorganic strengthened hydrogel membrane as regenerative periosteum. *ACS Applied Materials & Interfaces*, *9*(47), 41168–41180. https://doi.org/10.1021/acsami.7b13167

Xu, J., Zhang, Y., Xu, J., Liu, G., Di, C., Zhao, X., Li, X., Li, Y., Pang, N., Yang, C., Li, Y., Li, B., Lu, Z., Wang, M., Dai, K., Yan, R., Li, S., & Nie, G. (2019). Engineered nanoplatelets for targeted delivery of plasminogen activators to reverse thrombus in multiple mouse thrombosis models. *Advanced Materials*, *32*(4), e1905145, https://doi.org/10.1002/adma.201905145

Xu, Y., Han, X., Li, Y., Min, H., Zhao, X., Zhang, Y., Qi, Y., Shi, J., Qi, S., Bao, Y., & Nie, G. (2019). Sulforaphane mediates glutathione depletion via polymeric nanoparticles to restore cisplatin chemosensitivity. *ACS Nano*, *13*(11), 13445–13455. https://doi.org/10.1021/acsnano.9b07032

Yokoi, H., Kinoshita, T., & Zhang, S. (2005). Dynamic reassembly of peptide RADA16 nanofiber scaffold. *Proceedings of the National Academy of Sciences of the United States of America*, *102*(24), 8414–8419.

Yuan, C., Wang, P., Zhu, L., Dissanayaka, W. L., Green, D. W., Tong, E. H., & Zhang, C. (2015). Coculture of stem cells from apical papilla and human umbilical vein endothelial cell under hypoxia increases the formation of three-dimensional vessel-like structures in vitro. *Tissue Engineering Part A*, *21*(5–6), 1163–1172. https://doi.org/10.1089/ten.TEA.2014.0058

Zhao, Y., Yokoi, H., Tanaka, M., Kinoshita, T., & Tan, T. (2008). Self-assembled pH-responsive hydrogels composed of the RATEA16 peptide. *Biomacromolecules*, *9*(6), 1511–1518. https://doi.org/10.1021/bm701143g

Zhou, A., Chen, S., He, B., Zhao, W., Chen, X., & Jiang, D. (2016). Controlled release of TGF-beta 1 from RADA self-assembling peptide hydrogel scaffolds. *Drug Des Devel Ther*, *10*, 3043–3051. https://doi.org/10.2147/DDDT.S109545

Zigdon-Giladi, H., Khutaba, A., Elimelech, R., Machtei, E. E., & Srouji, S. (2017). VEGF release from a polymeric nanofiber scaffold for improved angiogenesis. *J Biomed Mater Res A*, *105*(10), 2712–2721. https://doi.org/10.1002/jbm.a.36127

How to cite this article: Zhang R, Liu Y, Qi Y, et al. Self-assembled peptide hydrogel scaffolds with VEGF and BMP-2 enhanced *in vitro* angiogenesis and osteogenesis. *Oral Dis*. 2022;28:723–733. https://doi.org/10.1111/odi.13785